

Controlled Growth of Carbon Nanotubes on Focus Ion Beam Patterned Substrates via Chemical Vapor Deposition

Blake Jon Rego^{*}, Papot Jaroenapibal[†], and David E. Luzzi[†]

^{*}*Department of Applied Physics, Columbia University, New York, New York 10027, USA*

[†]*Department of Materials Science and Engineering, University of Pennsylvania, Philadelphia, Pennsylvania 19104, USA*

Abstract

In this study, we investigate factors that lead to the controlled growth of single walled carbon nanotubes. The concentration of the catalyst solution, the effect of fast-heating vs. slow-heating, and the direction of the gas flow relative to tube growth were studied in respect to nanotube densities (number of nanotubes per gap) and nanotube orientation in the growth of single walled nanotubes across 4 μm gaps via chemical vapor deposition. Samples were characterized through the use of scanning electron microscope imaging. In the growth of nanotubes formed from iron/molybdenum nanoparticles, it is observed that the fast growth method produced a higher nanotube density than does the slow growth method. We also report that as concentration of the catalyst solution increases, the tendency of particles depositing on the substrate increases as well as the particles' tendency to agglomerate. Thus, the appropriate solution must have a catalyst concentration high enough such that enough particles are deposited on the substrate, but low enough such that agglomeration that causes surface diffusion does not have a dominant effect. The catalyst solution concentration that produced the highest nanotube density yield was 10mg $\text{Fe}(\text{NO}_3)_3$: 100 mL 2-Propanol. Moreover, there is also a noticeable morphology difference between the deposited catalyst particles from fast heating growth and particles from slow heating growth. We believe this difference to be due to thermal fluctuations caused by the fast-heating method as well as grain coarsening in the slow-heating method.

I. Introduction

In order to achieve the sensitivity level necessary for advanced sensing applications, current work is being done to reduce the size of mechanical resonators down to the nano scale. The applications of a nano resonator would include, but not be limited to, increased sensitivity mass sensors, chemical/biological sensors and/or high frequency oscillators. In biomedical systems, sensors would be useful at the nano

scale such that these systems can be implemented into the body without harming the patient¹. Another motivation of nano scale devices is that it can potentially minimize power consumption and reduce costs of devices¹.

The minimum force that a resonator can detect is given by the following equation²:

$$F_{\min} \sim \sqrt{\frac{wt^2}{lQ}}$$

In this equation w , t , l and Q are width, thickness, length and the quality factor respectively. Minimizing the detectable force means increasing the sensitivity of the device. One way to accomplish this is to manufacture resonators from stiff materials that have high aspect ratios (length compared to width/thickness). Yet the current surface machining technology only allows the fabrication of materials with the minimum lateral dimensions of 50 nanometers³. Alternatively, the unique structure of single-walled carbon nanotubes (SWNTs) offers an innovative platform upon which quality resonating systems can be designed. SWNTs have diameters reported as small as 0.7 nanometers⁴ as well as lengths as large as in the order of centimeters⁵. This potentially high aspect ratio makes nanotubes an excellent candidate material for a nano-resonator.

With the intent of fabricating nano resonators from carbon nanotubes, controlling the growth and direction is crucial for effective devices. Studies of mechanical properties of SWNTs have already begun via the investigations of mechanical resonance of nanotube bundles^{6, 7}. The goal of this study is to determine experimental factors that will lead to predictable SWNT properties. More specifically, we desire to find factors that will lead to the growth of straight (minimum defects) isolated SWNTs so that it can potentially be used as a nano resonator.

In order to reach these goals, we must determine what conditions control nanotube density and orientation. Previous studies on the concentration of the catalyst have found lower concentrations to yield more individual tubes⁸. Interestingly, in regards to orientation, there is contrasting literature over whether or not gas flow affects the growth direction of nanotubes^{9, 10}. Other studies have found that nanotube density can be controlled by varying the

thickness of layered catalyst metals¹¹. In our series of experiments, we look at the effect of gas flow on SWNT orientation, the effect of catalyst concentration on nanotube density, and the differences between the fast-heating and slow-heating growth methods on density and morphology of nanotubes.

II. Experimental

Preparation of the Substrate

An oval shaped molybdenum TEM gap (purchased from Ted Pelta Inc.) is cleaved along the long axis into two separate C-shaped halves. Each half was used as an individual substrate in the experiments. On each substrate, a focused ion beam (FEI DB235 FIB) is used to mill out individual gaps. The gaps were located on the inside arc of the C shaped substrate. On each substrate, ten gaps are milled and separated into four separate groups (see Figure 1). The pattern acts as a map to allow us to keep track of the sample such that the same sample can be found after subsequent processing steps. All gaps are four microns wide and within each group, each gap is separated by four microns. The nanotubes are to grow across these gaps, making bridges over them.

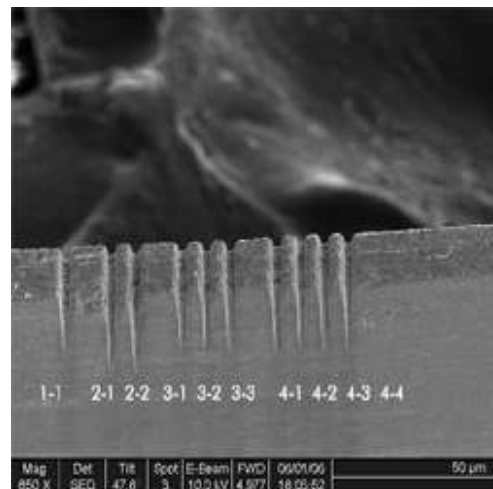


Figure 1 (previous page): Using the FIB, four groups of gaps are created for nanotube growth. The gaps are labeled by group and gap, starting with 1-1 on the far left to 4-4 on the far right. This picture was taken using SEM imaging.

Creation of the Catalyst

The catalyst solution is made from iron oxide $\text{Fe}(\text{NO}_3)_3$, molybdenum $\text{MoO}_2(\text{ACAD})$, aluminum oxide Al_2O_3 , and isopropyl alcohol. The actual catalyst nanoparticles will be a mixture of the iron nitrate and molybdenum oxide compound. It has been found that the combination of iron and molybdenum have synergistic effects when combined as a nanoparticle⁴. The motivation for including aluminum oxide in the solution is two fold for two main reasons. Firstly, the Fe/Mo nanoparticle will embed into the large porous alumina cluster, preventing the agglomeration of nanoparticles. Since the Fe/Mo particles are kept small, single walled nanotubes rather than rather than multi-walled carbon nanotubes (MWNT) are produced. In addition, alumina clusters will help produce isolated nanotubes, rather than bundles of them.

The ratio of iron oxide to molybdenum to aluminum oxide was kept fixed at 10:3:20 in every trial of the experiments. In the segment of the experiment in which the concentration of the catalyst was to vary, the amount of isopropyl alcohol was increased or decreased accordingly.

For a given concentration level, let X be the amount of isopropyl alcohol in mL desired in solution (The different possibilities of X will be discussed in the *Variable* portion of the experimental section). To create the catalyst, we first combine the iron oxide, molybdenum and X/2 isopropyl alcohol. This solution is stirred for two hours. Independently, we combine aluminum oxide and X/2 isopropyl

alcohol and stir for two hours. After the two hours are complete, we combine both solutions and allow them to mix overnight. The solution is typically used within 48 hours of its creation. An interval of time longer than this can cause agglomeration of the catalyst particles.

Depositing the Catalyst on the Substrate

The catalyst solution is next sonicated using a Branson 3510 Bath Sonicator for a minimum of 30 minutes. This is done to break agglomerated particles into smaller particles. The substrate is cleaned via a rinse with acetone, ethanol, and de-ionized water. After the substrate dries, it is submersed in the catalyst solution for exactly one minute. In order to maximize the probability of the catalyst particles to be deposited on the substrate, the substrate is then dried with the inside arc facing down, such that the solution drips down where the gaps are etched. Finally the substrate is placed into a hollow 4"-6" quartz tube (open at both ends) and is ready to be placed in the furnace.

Chemical Vapor Deposition

In this analysis, two methods of chemical vapor deposition are studied: the fast-heating method, and the slow-heating method. For both methods, the CVD setup that was used includes a home-built furnace and gas-flow chamber. In the slow heating method, the quartz tube containing the molybdenum substrate is placed in the center of the furnace and sealed. Argon gas is then flowed at 1500 standard cubic centimeters per minute (sccm) for 5 minutes to flush out the furnace. Hydrogen gas is then turned on at 400 sccm as the argon gas flow is turned off. The furnace is then ramped up to 900° C. Once 900° C is achieved, methane (CH_4) gas is flowed at

800 sccm into the furnace for fifteen minutes. After these fifteen minutes, the methane gas flow is turned off and the furnace is allowed to cool. To prevent oxidation of the tubes, the hydrogen gas continues to flow until the furnace reads temperatures of less than 100⁰ C.

In the fast-heating method, the quartz tube containing the substrate is placed within the chamber, but outside the heated region of the furnace. In a similar manner to the slow-heating method, the furnace is sealed and Argon gas is used to flush out the chamber at 1500 sccm for 5 minutes. Hydrogen gas is flowed at 400 sccm into the chamber as the temperature is ramped to 900⁰ C.

However, in the fast-heating method, the sample's temperature is not being ramped up as it is outside the heated region. Once 900⁰ C is achieved, the sample is pushed into the heated region of the furnace using a long quartz rod that protrudes outside the furnace. This rod is secured by an O-ring that prevents gas from leaking outside the chamber. The methane is allowed to flow at 800 sccm for 10 minutes. Once the 10 minutes are finished, the methane is turned off and the substrate furnace is allowed to cool, similar to the slow heating method.

Variables

The three main areas of exploration in this paper is the study of how concentration, gas flow direction, and slow vs. fast heating procedures affect carbon nanotube growth.

In order to study the effect of gas flow direction on nanotube growth, we aligned the etched gaps (desired nanotube growth direction) parallel and perpendicular to the direction of the gas flow. While varying the gas flow direction, all samples were tried under the slow growth

mechanism. In addition, the concentration of the catalyst solution was fixed to 10mg Fe(NO₃)₃ : 200 mL IPA.



Figure 2: A schematic diagram of the position of the substrate in relation to the gas flow direction. The growth of nanotubes was performed where the tubes that would bridge the gaps were aligned parallel (left) to the gas flow and perpendicular (right) to the gas flow.

In terms of concentration, the four conditions for nanotube growth were:

10mg Fe(NO₃)₃ : 400 mL IPA
 10mg Fe(NO₃)₃ : 200 mL IPA
 10mg Fe(NO₃)₃ : 100 mL IPA
 10mg Fe(NO₃)₃ : 50 mL IPA

While the concentration of the catalyst solution was being varied, the orientation of the substrates was kept constant: the desired nanotubes were parallel to the gas flow for all these trials. Under each of the four concentration conditions, the growth of the nanotubes was performed under the fast-heating and slow-heating methods. For every 10mg Fe(NO₃)₃, there is 3 mg of MoO₂(ACAD) and 20 mg of Al₂O₃. This ratio stays fixed throughout all trials.

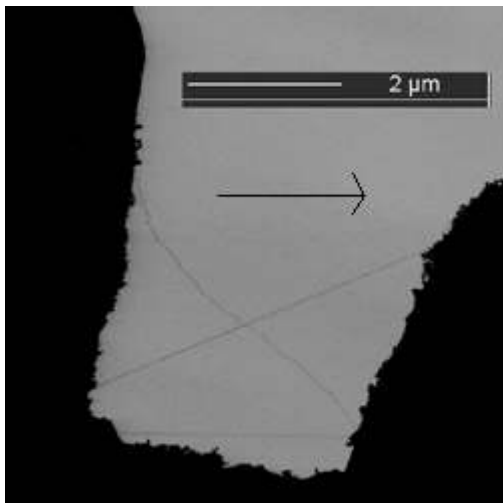
III. Results and Discussion

Gas Flow Direction

From previous studies performed on the fast-heating growth mechanism, if gas flow were to have an effect on nanotube growth, we were expecting the nanotubes to grow aligned with the gas flow direction⁹. However, in our own experiments, there was no indication that gas flow direction had any effect on the growth of the nanotubes in

either the slow-heating or fast-heating growth mechanisms.

a)



b)

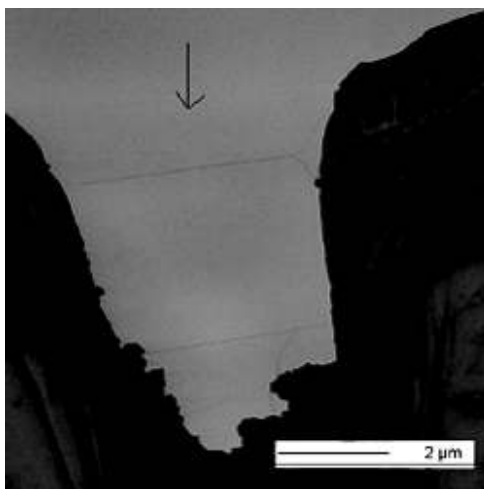


Figure 3a (above): SEM image of a gap with catalyst concentration of 10mg Fe (NO₃)₃: 200 mL IPA. The gas flow was aligned parallel to the desired tube growth (in the direction of the arrow).

Figure 3b (below): SEM image of a gap with the same concentration as Figure 3a. The gas flow direction was aligned perpendicular to the desired tube growth (in the direction of the arrow).

In Figure 3a, observe the various directions the nanotubes grow in order to bridge the gap. For the duration of the growth period, methane gas (the carbon source) is flowed constantly at 800 sccm in the direction of the

arrow. If the gas flow direction were too affect the SWNT growth, the tubes should exhibit straight morphologies, each nanotube parallel to its neighbor. Clearly, this is not the case.

Moreover, in Figure 3b, with the gas flow aligned perpendicular to the desired tube growth, nanotubes still managed to make their way across the gaps. Of exactly 10 gaps studied in each of the two conditions, the average tube density was 1.5 tubes per gap for the parallel orientation and 1.2 tubes per gap for the perpendicular orientation. This further supports the notion that gas flow direction does not influence the growth of SWNTs.

The reason for the discrepancy between these results and the results found by Huang et al. could be the gas flow rate. The flow rate used in our experiments was 800 sccm of CH₄ and 400 sccm of H₂. The flow rate was not mentioned in Huang's paper⁹. Further research varying the gas speed must be performed in order to clear up the inconsistency between these experimental results. In another study done on gas flow direction and carbon nanotube growth by Li et al. at UC Irvine, nanotubes were found to grow with and against the flow direction¹⁰. These results are in concord with our own observations. In the experiments done by Li, the gas flow rate of their carbon source (CH₄) was 1000 sccm, similar to ours.

Concentration of the Catalyst Solution

The growth of nanotubes seems to be highly dependent on the catalyst solution concentration. Generally, as the concentration of the catalyst solution increases, the number of nanotubes increases. In order to quantify the results, the number of tubes was hand counted off SEM imaged photos of the sample gaps taken after the completed chemical vapor

deposition process. Figure 4 enumerates these results according to catalyst concentration.

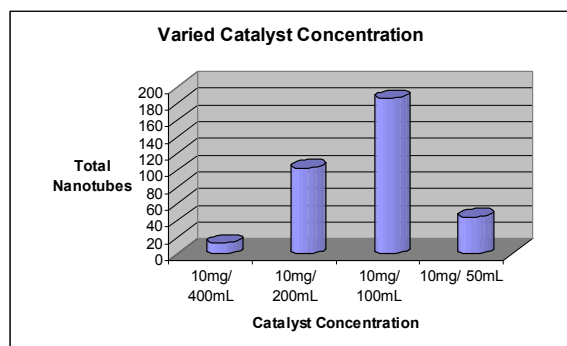


Figure 4: This graph depicts the number of nanotubes grown under each of the four tested catalyst solution concentrations. Each concentration level had exactly 20 different sample gaps.

With higher concentrations of catalyst particles in solution, more of the catalyst particle deposits on the surface of the substrate, which subsequently results in higher counts of nanotubes.

In the lowest concentration solution, nanotubes grew in only 3 of the 20 possible gaps. In the next two batches of samples, the amount of nanotubes increased markedly as the concentration rose, consistent with the idea that higher concentrations allow for increased catalyst particle deposition, which increases the number of tubes found within a gap. However, notice the dramatic drop off in nanotubes between the 10mg $\text{Fe}(\text{NO}_3)_3$: 100 mL IPA and the 10mg $\text{Fe}(\text{NO}_3)_3$: 50 mL IPA. The highest concentration of catalyst solution we tested seems to have surpassed a critical threshold for carbon nanotube growth.

After examining the SEM images taken of sample gaps from the highest concentration solution, it is clear that the reason that nanotube growth is impeded at this concentration is due to catalyst particles agglomerating and partially to completely filling the gaps between the gaps themselves. In some cases, the catalyst particles may even fill in the entire gap with

catalyst particles, leaving little, if any room for the nanotubes to grow. For an example of this phenomenon, see Figure 5. In fact, as seen in Figure 6, the number of gaps that are completely filled by catalyst particles increases as concentration increases.

However, this is not the main reason for the inhibition of nanotube growth. As concentration increases, the catalyst particles have a higher tendency to agglomerate, forming larger particles. When the catalyst particle is too large, the possibility for bulk diffusion of carbon atoms into the catalyst particle is lower, thus decreasing the probability for nucleation. Instead of bulk diffusion, surface diffusion would then become a dominate effect. Surface diffusion, unlike bulk diffusion, leads into graphene sheets that wrap around the catalyst particle, rather than a nucleation site that would lead to a carbon nanotube.

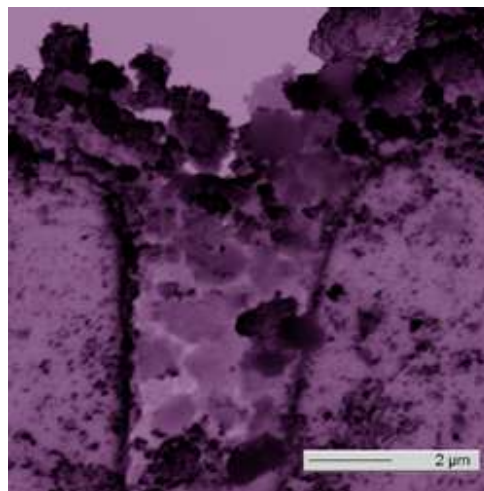


Figure 5: SEM image of a gap grown under fast-heating conditions with catalyst concentration of 10mg $\text{Fe}(\text{NO}_3)_3$: 50 mL IPA. The catalyst particles have completely filled the gap, leaving no room for SWNT growth.

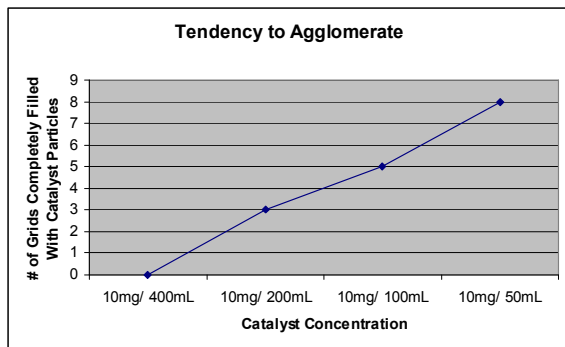


Figure 6: This graph shows the number of gaps that were completely filled by catalyst particles as a function of catalyst concentration. In these gaps, no nanotubes were able to grow.

To recap, if the concentration of the catalyst particle solution is too low, nanotubes tend not to grow because there is too few catalyst particles deposited on the substrate. On the contrary, if the catalyst concentration solution is too high, the catalyst particles have higher propensity agglomerate, which leads to surface diffusion rather than bulk diffusion. In turn the probability for a nucleation site is diminished, and a graphene catalyst particle coating, rather than a nanotube is formed. Thus we learn that the optimal concentration for nanotube growth is somewhere in between.

The “optimal” concentration for the catalyst particle solution depends on what or how one intends to study/utilize the nanotubes. The highest number of nanotubes was created at the 10mg Fe (NO₃)₃ : 100 mL IPA. The average nanotube density at this particular concentration was 9.3 nanotubes per gap. Although this concentration is the best for number of tubes, it is not ideal for making devices. For devices, one would want nanotubes to be grown consistently, but in a low enough density such that there would be tubes in isolation. This way, one can use a tube as a nano resonator, and/or study its properties. The best concentration for these conditions is Fe (NO₃)₃ : 100 mL IPA. The average nanotube density is 5.15

nanotubes per gap and only three of the twenty gaps were left without nanotubes after all experiments.

Fast Heating Growth vs. Slow Heating Growth

Generally, it is observed that the fast-heating growth mechanism produces more tubes than the slow-heating mechanism does. The contrast between the nanotube densities in the fast-heating and slow-heating mechanisms can be seen qualitatively in Appendix A or in graph form in Figure 7. We believe that this impeded growth is due to a phenomenon called grain coarsening that occurs exclusively during the slow-heating mechanism. As the substrate is annealed, the catalyst particles, which behave like a random grain structure, will become unstable and the unbalanced forces will cause the boundaries to migrate towards their centers of curvature. The overall result of this boundary migration will be to increase the mean grain size and reduce the total grain boundary energy¹². As the particles increase in size, the particles have a lower probability for a nucleation site for similar reasons to why agglomeration impedes nanotube growth. Surface diffusion, rather than bulk diffusion will play the dominant role and graphene sheets will grow around the catalyst particle. The substrates in the fast-heating method do not experience grain coarsening effects as much because of the speed at which the substrate is heated. This may explain why the fast-heating mechanism produces on average more tubes than the slow-heating mechanism.

In addition to the clear difference in nanotube density that is exhibited between the slow-heating method and the fast-heating method, there is also a noticeable morphology variation between the catalyst particles in each method. For an example of

this phenomenon, compare figures A1 and A5 or A3 and A7 in the Appendix. This morphology difference can be attributed to the coarsening that enlarges the catalyst particles in the slow-heating method, as well as the thermal fluctuations that take place during the fast-heating process. Coarsening, as mentioned previously, causes the catalyst particles to become larger and coated with graphene layers. In the fast-heating process, after the furnace has been heated to 900° C and the substrate has been placed into the furnace, the molybdenum substrate will heat up at a different rate as the surrounding air.

This difference in heating rates will cause a convection current, lifting the catalyst particles up off of the substrate and through the air⁵. The catalyst particles consequently move about more freely and are deposited sometimes even between the gaps. It is proposed that Huang et al. that the nanotubes that grow during the fast-heating method are via a mechanism called kite-growth⁹. This means that as the catalyst particles are flying through air due to the thermal fluctuations, nanotubes grow from a nucleation site behind it. In a way the nanotube is pushing the catalyst further out into the gap, rather than growing out from the particle. It can be described as a ‘tail’ that is growing from the catalyst particle as it moves about into and around the gap.

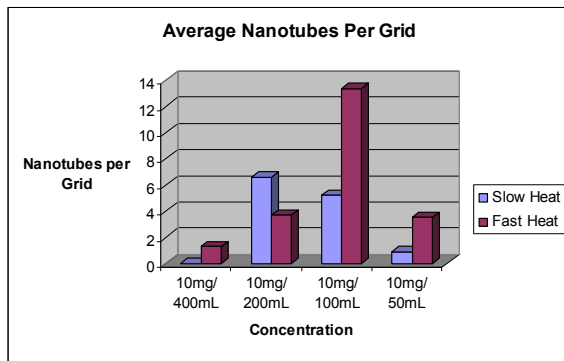


Figure 7: This graph exhibits the average number of tubes observed as concentration and growth rate vary.

IV. Conclusions

Although additional work is needed to hone the control of the nanotubes, much can be learned from the preceding experiments. At a flow rate of 800 sccm, the gas flow direction does not significantly affect the nanotube growth orientation. However, future work that varies the flow rate is necessary to see what gas speed, if any, will allow for control of nanotube orientation via flow direction.

In addition, it is observed that catalyst particle density has a pivotal effect on the nanotube density, in nanotubes per grid, of a substrate. As concentration of the catalyst particle solution increases, the amount of catalyst particles that is deposited on the substrate increases, which increases the nanotube density. Thus, catalyst concentration solutions that are too low do not have many tubes because there is not enough catalyst particles deposited on the surface on the substrate. However, agglomeration also increases as concentration increases. When agglomeration becomes too high, surface diffusion, rather than bulk diffusion dominates, decreasing the probability for a nanotube nucleation site. Therefore, if the concentration of the catalyst solution is too high, nanotube density is low because the excess agglomeration impedes growth.

It has also been observed that there is a morphology difference between the catalyst particles of slow-heating and fast-heating particles. Coarsening causes the enlargement of catalyst particles and encourages graphene sheets to be wrapped around them. The fast-growth method is prone to thermal fluctuations and cause erratic deposition of catalyst particles between the tubes. In addition, there are generally more tubes grown with the fast-heating method than the slow-heating method.

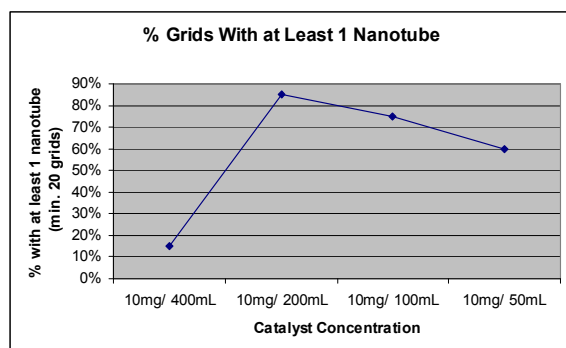


Figure 8: This graph shows the percentage of gaps that have at least one nanotube.

Speaking in terms of devices, the best concentration and heating mechanism would be the 10mg $\text{Fe}(\text{NO}_3)_3$: 200 mL IPA under slow-heating mechanism. While the 10mg $\text{Fe}(\text{NO}_3)_3$: 200 mL IPA have the highest tube density, the tubes are too many and too close together to make good resonators. Moreover, Figure 8 shows the percentage of gaps in each concentration that has at least one nanotube. The 10mg: 200 mL solution has the highest success rate. The reason we believe the slow-heating mechanism would be superior to the fast-heating mechanism for the purpose of building devices is because fast-heating causes the unpredictable deposition of catalyst particles within a given gap.

Figure 9 shows a gap that has nanotubes that could potentially be used as nano resonators. Until examined under a transmitting electron microscope (TEM), it is uncertain whether these are individual nanotubes or nanotube bundles. Nanotubes A and D are isolated, straight and with few noticeable defects. Although nanotubes B, C and E have straight morphology, they are possibly crossed with other nanotubes.

We have demonstrated that by controlling the growth mechanism and catalyst concentration, we can increase the probability of growing nanotubes that could be implemented in devices.

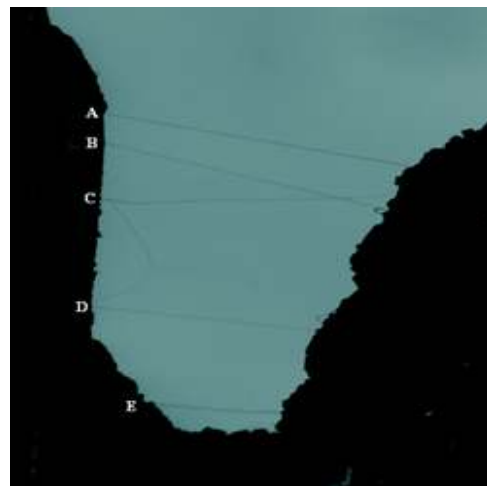


Figure 9: Gap grown under catalyst concentration of 10mg $\text{Fe}(\text{NO}_3)_3$: 200 mL IPA with some nanotubes that could serve as potential resonators.

V. Acknowledgements

I would like to give special thanks to Papot Jaroenapibal for his help and guidance throughout the entire duration of my project. Through his support, I have learned a tremendous amount about the science of nano-technology and the mindset required to be successful in graduate school. I would also like to express gratitude to Professor David E. Luzzi for giving me the opportunity to work in his laboratories and with his group members. I would like to thank all the group members for making me feel welcome and offering suggestions when needed. I want to thank Dr. Andrew McGhie for organizing the program, including all events and lectures for the REU students throughout the summer. I would like to acknowledge that this work utilized central facilities of the Penn Regional Nanotechnology. Finally I would like to recognize NSF, LRSM and MRSEC for the financial and organizational support that makes this entire program possible. This summer REU program was extremely rewarding and I look forward to applying to a similar program next year. Also, special thanks to Brian Tovar, for his valuable insight and opinions.

Appendix A – SEM Images of Sample Gaps

Slow Heating Method



Figure A1-10mg $\text{Fe}(\text{NO}_3)_3$: 400 mL IPA



Figure A2-10mg $\text{Fe}(\text{NO}_3)_3$: 200 mL IPA

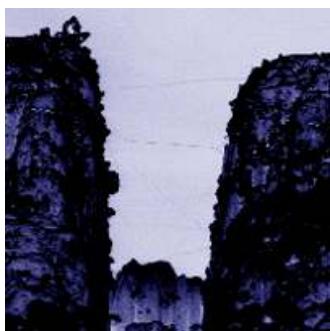


Figure A3-10mg $\text{Fe}(\text{NO}_3)_3$: 100 mL IPA



Figure A4-10mg $\text{Fe}(\text{NO}_3)_3$: 50 mL IPA

Fast Heating Method



Figure A5-10mg $\text{Fe}(\text{NO}_3)_3$: 400 mL IPA

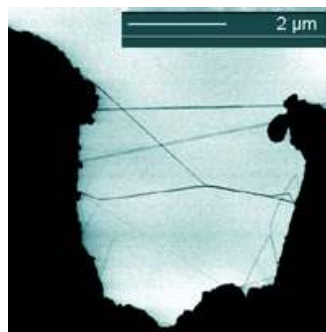


Figure A6-10mg $\text{Fe}(\text{NO}_3)_3$: 200 mL IPA



Figure A7-10mg $\text{Fe}(\text{NO}_3)_3$: 100 mL IPA

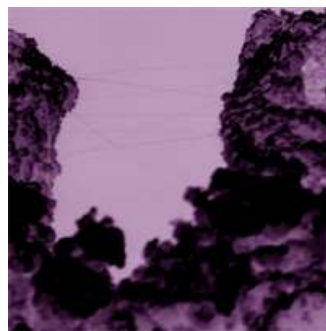


Figure A8-10mg $\text{Fe}(\text{NO}_3)_3$: 50 mL IPA

¹ *From Micro- to Nanosystems: mechanical sensors go nano.* Hiercold, C. Journal of Micromechanics and Microengineering. Issue 9. September 2004. Zurich, Switzerland.

² K. Y. Yasumura, T. D. Stowe, E. M. Chow, T. Pfafman, T. W. Kenny, B. C. Stipe, and D. Rugar, IEEE J. MEMS **9**, 117 (2000).

³ H. G. Craighead, Science **290**, 1532 (2000).

⁴ *CVD Synthesis of Single Wall Nanotubes under "Soft" Conditions.* Harutyunyan, A., Pradhan, B. K., Kim, U. J., Chen, G., and Eklund, P. C. The Pennsylvania State University. *Nano Letters*, **2** (5), 525 -530, 2002.

⁵ *Direct Synthesis of Long Single-Walled Carbon Nanotube Strands.* Zhu, H. W., Xu, C. L., Wu, D. H., Wei, B. Q., Vajtai, R., Ajayan, P. M., Science. 0036-8075, May 3, 2002, Vol. 296, Issue 5569

⁶ *Transmission-Electron-Microscopic Studies of mechanical properties of Single-Walled Carbon Nanotube Bundles.* Jaroenapibal, P., Luzzi, D. E., and Evoy, S. University of Pennsylvania. Applied Physics Letters. November 8, 2004. Volume 85, Number 19.

⁷ *Electrostatic Deflections and Electromechanical Resonances of Carbon Nanotubes.* Poncharal, P., Wang, Z. L., Ugarte, D., and de Heer, W. A. Science, vol. 283, pp. 1513-1516, March 1999.

⁸ *Direct Growth of Single-Walled Carbon Nanotube Scanning Probe Microscopy.* Cheung, C., Hafner, J., Odom, T. W., Kim, K., and Lieber, C. Nature [0028-0836] Hafner. 1996, vo. 384 pg. 147.

⁹ *Growth Mechanism of Oriented Long Single Walled Carbon Nanotubes Using "Fast-Heating" Chemical Vapor Deposition Process.* Huang, S., Woodson, M., Smalley R., and Liu, J. Nano Letters. Duke University. April 4, 2004, Vol. 4, No. 6 pgs. 1025-1028.

¹⁰ *Electrical Properties of 0.4 cm Long Single-Walled Carbon Nanotubes.* Li, S., Yu, Z., Rutherglen, C., and Burke, P. University of California, Irvine. *Nano Letters*, **4** (10), 2003 -2007, 2004.

¹¹ *Multilayered Metal Catalysts for Controlling the Densities of SWCNT Growth.* Delzeit, L., Chin, B., Cassel, A., Stevens, R., Nguyen, C., and Meyyappan,

M. Chemical Physical Letters. Vol. 348 16 November 2001. pp. 368-374.

¹² *Thermally Activated Migration of Grain Boundaries.* Porter, D. A., Easterling, and K. E., Phase Transformations in Metals and Alloys. 2nd Ed. Chapman and Hall Publishing. London 1992.